Multi-scale Discontinuities Due to Differential Stress Around a Pressurized Borehole

Hao Xu[1], Chloe Arson[2], and Seth Busetti[3]

[1]Ph.D. student, School of Civil and Environmental Engineering, Georgia Institute of Technology, Atlanta, GA, 30332; PH (979) 777-9511; EMAIL: haoxu@gatech.edu
[2]Assistant Professor, Ph.D., School of Civil and Environmental Engineering, Georgia Institute of Technology, Atlanta, GA, 30332; PH (404)385-0143; EMAIL: chloe.arson@ce.gatech.edu
[3]Senior Geomechanicist, Ph.D., ConocoPhillips, Structure & Geomechanics group, Houston, TX; EMAIL: seth.busetti@conocophillips.com

ABSTRACT: Most fracture propagation models do not properly represent smaller-scale discontinuities in the process zone. This paper reviews the different modeling strategies available to date to model crack propagation at microscopic, mesoscopic and macroscopic scales. The Differential Stress Induced Damage (DSID) model recently proposed by the authors (Xu and Arson, 2014) is then used to simulate fracture propagation around a pressurized borehole with the Finite Element Method. In a pristine rock mass, the damage zone presents several symmetries in three dimensions, which are in agreement with the definition of the damage-driving force controlling the initiation and propagation of damage. If hydraulic fracturing is enhanced by the presence of initial cracks, the propagation of the damage zone depends on the geometry of the initial defects. It is found that simulating rock initial texture by a smeared damaged zone provides good analogs to the viscosity-dominated and toughness-dominated fracture propagation regimes expected during hydraulic fracturing. Future work will be dedicated to the fully coupled formulation of a hydro-mechanical model of damage around hydraulic fractures.

INTRODUCTION

Cavities, faults and fractures are usual "large-scale" discontinuities in geotechnical engineering (i.e., meter to kilometer scale). Among those, "fractures" usually refer to Griffith macroscopic cracks, opening under the influence of a differential stress (Florez-Nino, 2005). For instance, fracture nucleation and propagation are of interest tunnel excavation (Excavation Damaged Zone), geothermal energy extraction and hydraulic fracturing processes (Tsang et al., 2005; Lund, 2007; Adachi et al., 2007). In numerical codes, large-scale discontinuities such as hydraulic fractures and faults are usually modeled as separated surfaces or weakly bonded surfaces, or are represented

with notch shapes at the macro-scale. Most fracture propagation models either neglect the presence of smaller-scale discontinuities in the process zone (also called damaged zone in the following), or represent them in the form of a plastic zone (Liu, 1984). Neglecting the effects of micro-cracks leads to ignore the degradation of solid stiffness, and therefore, to under-estimate fracture propagation. Moreover, the non-uniform distribution of micro-cracking makes it difficult to upscale the evolution of flaws at the scale of a Representative Elementary Volume (REV – Lemaitre and Desmorat, 2005). A representation of rock microstructure, finer than an averaged plastic zone, is needed to relate the extent of the damaged zone to the density, size and shape of the cracks. Recent studies established an explicit relationship between rock grain size distribution (GSD) and the dimensions of the fracture process zone (Tarokh and Fakhimi, 2013), which illustrates the importance of relating rock fabric to rock stiffness in the surrounding of large-scale discontinuities. Continuum Damage Mechanics (CDM) provides a theoretical framework to relate geometrical fabric tensors to stiffness, and therefore, predict damaged rock mechanical properties (Colovos et al., 2013). In this paper, the Differential Stress Induced Damage (DSID) model recently proposed by the authors (Xu and Arson, 2014) is used to simulate fracture propagation around a pressurized borehole with the Finite Element Method (FEM). The first section of this paper reviews the different modeling strategies available to date to model crack propagation at microscopic, mesoscopic and macroscopic scales. The second section presents the thermodynamic framework of the DSID model, and explains how the DSID model indirectly couples the micro- and meso- scales. The damage variable is a second-order tensor, similar to Oda's fabric tensor (Oda, 1984; Cowin, 1985). The DSID model allows modeling the initiation and propagation of cracks several orders of magnitude smaller than the large-scale discontinuities originating the damaged zone. The DSID model was implemented in *ABAQUS* Finite Element software. The influence of initial rock structure on hydraulic fracture propagation is studied in Section 3, which presents results obtained for the same borehole pressurization problem, in the absence of initial damage (case 1), in the presence of a notch at the wellbore wall (case 2), and in the presence of an initial smeared damaged zone (case 3).

DAMAGE MODELING ACROSS THE SCALES – OVERVIEW

At the macro-scale, fracture propagation can be simulated with Finite Element Methods (FEM) and Extended Finite Element Methods (XFEM). For multiple fractures however, such continuum-based approaches become time consuming. On the other hand, Discrete Fracture Network (DFN) models focus on fracture apertures; the behavior of rock matrix outside the fractures is accounted for indirectly, through rock/fracture interface rheological laws. Fracture coalescence remains a challenge in most numerical models. Fracture propagation at the macroscale (meter to kilometer scale) and at the microscale (micron to millimeter scale) can be predicted within the framework of fracture mechanics (with stress intensity factors involved in the expression of propagation thresholds). In between, subsets (or families) of micro-cracks define "damage" at the meso-scale, and are best represented by Continuum Damage Mechanics (CDM) models (Table. 1).

Table 1. Damage Modeling Across the Scales
An Overview of theoretical frameworks and numerical methods.

Micro-scale	Meso-scale	Macro-scale
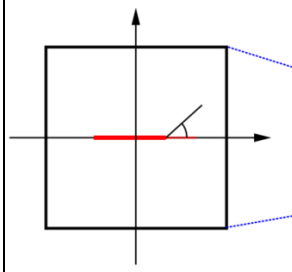	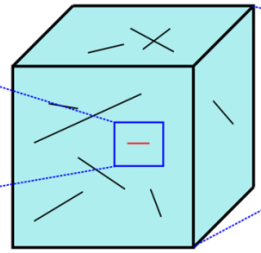	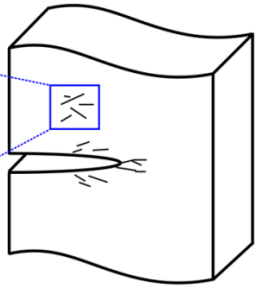
Micro-mechanics, Linear Elastic Fracture Mechanics (LEFM), Discrete Element Method (DEM)	Continuum Damage Mechanics (CDM), Finite Element Method (FEM)	LEFM, FEM, Extended FEM, Cohesive Zone Method (CZM)
1. $\xi_\alpha = (r_\alpha, \mathbf{n}_\alpha)$ 2. $\frac{\partial g_\alpha}{\partial r_\alpha} = \mathcal{G}_\alpha^C$ 3. $f_d(g_\alpha^n, g_\alpha^t) = 0$ (Swoboda & Yang, 1999; Dormieux, 2006)	1. $\mathrm{F}^{(\mathrm{p})} = \frac{\pi}{4}\frac{1}{V_{REV}}\sum_{\alpha=1}^{N}(r_\alpha, \mathbf{n}_\alpha)$ **2.** $\dot{\mathbf{D}} = \mathbf{J}:\mathbf{Y}$ 3. $\mathbf{Y} = -\frac{\partial \Psi^*}{\partial \mathbf{D}}$ and $\dot{D} = \dot{\lambda}\frac{\partial Q(\mathbf{D},\mathbf{Y},\mathcal{F})}{\partial \mathbf{Y}}$ (Oda, 1984; Swoboda & Yang, 1999)	1. $\mathcal{K} = K'\left(\frac{t^2}{\mu'^5 Q_0^3 E'^{13}}\right)^{1/18}$ 2. $\frac{\partial w}{\partial t} = \frac{1}{12\mu}\frac{1}{r}\frac{\partial}{\partial r}\left(rw^3\frac{\partial p}{\partial r}\right)$ (Savitski & Detournay, 2002)

1. Micro-scale

At the micro-scale, the size and orientation of discontinuities are predicted within a micro-mechanical framework. For instance, crack growth in mode I is predicted by using Griffith criterion: crack length is work-conjugate a "damage driving force" called "affinity" or "energy release rate"; the crack is unstable if the energy release rate exceeds a certain threshold depending on stress concentration factors.

2. Macro-scale

In macro-scale, Linear Elastic Fracture Mechanics (LEFM) is often utilized to analyze critical states of the material, but it mainly focuses on isolated discontinuities. There is no dissipation potential involved, and fracture propagation is predicted by solving Partial Differential Equations (PDEs) coupling fracture length and aperture to pressure. There is no macroscopic damage threshold. Several numerical methods may be employed, mainly FEM, XFEM and CZM (Cohesive Zone Method - Carrier and Granet, 2012). In all of these methods however, fracture nucleation is impossible to predict, and the expected (approximate) position of the fracture has to be postulated.

3. Meso-scale

The meso-scale lies between the micro- and macro-scale. This is basically the scale of observation, at which phenomena are modeled within a continuum-based framework. In CDM, the mesoscopic damage evolution law can be expressed at the scale of a Representative Elementary Volume (REV), by upscaling a microscopic fracture

mechanics model. For instance, the model proposed by Swoboda & Yang (1999) allows relating microscopic affinities to mesoscopic stress for a finite number of crack sets characterized by a crack radius and a plane normal vector. Swoboda & Yang's framework can be extended to relate the mesoscopic stress to the statistical distributions of micro-crack size and orientation. Oda (1984) and Lubarda & Krajcinovic (1993) related defined micro-crack density and orientations to a mesoscopic fabric tensor. Cowin (1985) related the fabric tensor to the elastic stiffness tensor without resorting to any sort of homogenization scheme. Maleki & Pouya (2010) found an empirical statistics-based relationship between Oda's fabric tensor (1984) and the mesoscopic permeability tensor, and also related the fabric tensor to the mesoscopic damage tensor – i.e., the damage tensor used as a dissipation variable in a CDM model. As mentioned earlier, mesoscopic damage is of interest for the study of Excavation Damage Zones (EDZ) and fracture process zones, which involves coupling the evolution of a large-scale discontinuity to the evolution of smaller-scale discontinuities. LEFM parameters, such as fracture toughness and Stress Intensity Factor(s), have to be adapted to account for the damaged state of the rock mass (Valko and Economides, 1994). The expressions of stress intensity factors and toughness of the undamaged matrix are usually adapted by replacing stress by "effective stress" (the fictitious stress that would be developed in an undamaged REV to store the deformation energy of the damaged REV subject to real stress). This relatively simple modeling assumption allows deriving "damaged toughness" and other damaged LEFM parameters simply by substituting the elastic properties of the intact (undamaged) rock mass by the damaged elastic properties. The position of the crack tip and the stress field can then be predicted by using the resulting LEFM equations, modified to account for damage.

OUTLINE OF THE DIFFERENTIAL STRESS INDUCED DAMAGE MODEL

The Differential Stress Induced Damage (DSID) model (Xu and Arson, 2014) allows predicting mechanical anisotropy induced by a reorientation of stress principal directions in the rock mass (change of differential stress). CDM is used to predict the statistical average response of the cracked rock, without describing the real geometry of each micro-crack. The damage variable introduced by Kachanov (1992) is used to predict damage-induced anisotropy of deformation and stiffness. This variable is similar to Oda's fabric tensor (1984). The DSID model allows predicting directional micro-crack propagation around pressurized discontinuities such as boreholes and fractures. This is a promising feature, because previous damage models used in numerical methods to study hydraulic fracturing were limited to scalar damage (Valko and Economides, 1994) or flat debonded surfaces (which cannot conduct fracture flow – Suzuki, 2012). In addition, the DSID model distinguishes tension and compression damage thresholds, while previous theoretical frameworks were not solving problems related to the non-differentiability (and associated numerical issues) of damage variables depending on absolute values. Multiple mechanisms (including crack propagation in tension and compression for instance) are most often modeled by coupling damage and plastic potentials (Cicekli, 2007), which tremendously increases the model complexity and the number of material parameters involved. In the proposed model, emphasis is put on the dependence of anisotropic crack propagation to

differential stress. The thermodynamic framework of the DSID model is summarized in Table 2. Stress/strain relationships are derived from the expression of a free energy potential. Damage evolution is controlled by a damage function, similar to Drucker-Prager yield function (but depending on the energy release rate). The damage flow rule is non-associate, and the damage potential is chosen so as to ensure the positivity of dissipation associated to damage. The irreversible deformation due to damage follows an associated flow rule, which allows representing physical anisotropic trends of the deformation tensor during the damage process. More details are provided in (Xu and Arson, 2014).

Table 2: Thermodynamic framework of the DSID model.

	D.S.I.D. Model
1. Free Energy	$G_s(\boldsymbol{\sigma},\boldsymbol{\Omega}) = \frac{1}{2}\boldsymbol{\sigma}:\mathbb{S}_0:\boldsymbol{\sigma} + a_1\mathrm{Tr}\boldsymbol{\Omega}(\mathrm{Tr}\boldsymbol{\sigma})^2 + a_2\mathrm{Tr}(\boldsymbol{\sigma}\cdot\boldsymbol{\sigma}\cdot\boldsymbol{\Omega}) + a_3\mathrm{Tr}\boldsymbol{\sigma}\,\mathrm{Tr}(\boldsymbol{\Omega}\cdot\boldsymbol{\sigma}) + a_4\mathrm{Tr}\boldsymbol{\Omega}\,\mathrm{Tr}(\boldsymbol{\sigma}\cdot\boldsymbol{\sigma})$
	$\boldsymbol{\epsilon}^E = \frac{\partial G_s}{\partial \boldsymbol{\sigma}} = \frac{1+\nu_0}{E_0}\boldsymbol{\sigma} - \frac{\nu_0}{E_0}(\mathrm{Tr}\boldsymbol{\sigma})\boldsymbol{\delta} + 2a_1(\mathrm{Tr}\boldsymbol{\Omega}\,\mathrm{Tr}\boldsymbol{\sigma})\boldsymbol{\sigma} + a_2(\boldsymbol{\sigma}\cdot\boldsymbol{\Omega}+\boldsymbol{\Omega}\cdot\boldsymbol{\sigma}) + a_3[\mathrm{Tr}(\boldsymbol{\sigma}\cdot\boldsymbol{\Omega})\boldsymbol{\delta} + (\mathrm{Tr}\boldsymbol{\sigma})\boldsymbol{\Omega}] + 2a_4(\mathrm{Tr}\boldsymbol{\Omega})\boldsymbol{\sigma}$
	$\mathbf{Y} = \frac{\partial G_s}{\partial \boldsymbol{\Omega}} = a_1(\mathrm{Tr}\boldsymbol{\sigma})^2 + a_2\boldsymbol{\sigma}\cdot\boldsymbol{\sigma} + a_3\mathrm{Tr}(\boldsymbol{\sigma})\boldsymbol{\sigma} + a_4\mathrm{Tr}(\boldsymbol{\sigma}\cdot\boldsymbol{\sigma})\boldsymbol{\delta}$
2. Damage Function	$f_d = \sqrt{J^*} - \alpha I^* - k$
	$J^* = \frac{1}{2}\left(\mathbb{P}_1:\mathbf{Y} - \frac{1}{3}I^*\boldsymbol{\delta}\right):\left(\mathbb{P}_1:\mathbf{Y} - \frac{1}{3}I^*\boldsymbol{\delta}\right), I^* = (\mathbb{P}_1:\mathbf{Y}):\boldsymbol{\delta}$
	$\mathbb{P}_1(\boldsymbol{\sigma}) = \sum_{p=1}^{3}\left[H\left(\sigma^{(p)}\right) - H\left(-\sigma^{(p)}\right)\right]\mathbf{n}^{(p)}\otimes\mathbf{n}^{(p)}\otimes\mathbf{n}^{(p)}\otimes\mathbf{n}^{(p)}$
	$k = C_0 - C_1\,\mathrm{Tr}(\boldsymbol{\Omega})$
3. Damage Potential	$g_d = \sqrt{\frac{1}{2}(\mathbb{P}_2:\mathbf{Y}):(\mathbb{P}_2:\mathbf{Y})} - C_2$
	$\mathbb{P}_2(\boldsymbol{\sigma}) = \sum_{p=1}^{3} H\left[\max_{q=1.2,3}\left(\sigma^{(q)}\right) - \sigma^{(p)}\right]\mathbf{n}^{(p)}\otimes\mathbf{n}^{(p)}\otimes\mathbf{n}^{(p)}\otimes\mathbf{n}^{(p)}$
4. Flow Rules	$\dot{\boldsymbol{\epsilon}}^{id} = \dot{\lambda}_d\frac{\partial f_d}{\partial \boldsymbol{\sigma}} = \dot{\lambda}_d\frac{\partial f_d}{\partial \mathbf{Y}}:\frac{\partial \mathbf{Y}}{\partial \boldsymbol{\sigma}}$
	$\dot{\boldsymbol{\Omega}} = \dot{\lambda}_d\frac{\partial g_d}{\partial \mathbf{Y}}$

G_s: Gibbs free energy	$\mathbb{S}_0$: Undamaged compliance tensor	$\boldsymbol{\delta}$: Kronecker delta
$\boldsymbol{\sigma}$: Stress tensor	$\boldsymbol{\epsilon}^E$: Total elastic strain	E_0: young's Modulus
$\boldsymbol{\Omega}$: Damage variable	ν_0: Poisson's ratio	$\mathbf{Y}$: Damage driving force
f_d: Damage function	C_0: Initial damage threshold	$H(\cdot)$: Heaviside function
$\mathbb{P}_1$ and $\mathbb{P}_2$: Projection tensor	$\dot{\boldsymbol{\Omega}}$: Damage rate	$\dot{\lambda}_d$: lagrangian Multiplier
max(·): Maximum function	g_d: Damage potential	$\dot{\boldsymbol{\epsilon}}^{id}$: Irreavisible strain rate
a_1, a_1, a_1, a_1, α: Material parameters	$\sigma^{(p)}$ and $\mathbf{n}^{(p)}$: Principal stress and corresponding direction	C_1: Damage hardening variable

SIMULATION OF DAMAGE INDUCED BY PRESSURIZATION

The DSID model was implemented in *ABAQUS* Finite Element software, using a *UMAT* subroutine. A pure mechanical process of hydraulic fracturing is simulated, by

assuming that a high-pressure gas is injected into the rock mass on a localized portion of a wellbore. The domain under study is a cylinder 20m in diameter, and 20m in height. The borehole's diameter is 2m. External and internal boundaries are subjected to a normal pressure of 4MPa, except on a localized zone of thickness 0.2m on the inner surface of the borehole. Former work by Halm and Dragon (1998) and Shao et al. (2005) is used to get a set of damage constitutive parameters calibrated against experimental rock mechanics test results. The parameters chosen in the simulations are typical of a granite (Table. 3). In the following figures, *UMAT* parameter "SDV25" stands for f_d; therefore a non-negative value of SDV25 indicates that the element is experiencing damage.

Table 3. Parameters Used in the Simulations with the Proposed Damage Model.

E_0 GPa	ν_0	a_1 $\times 10^{-4}\text{GPa}^{-1}$	a_2 $\times 10^{-4}\text{GPa}^{-1}$	a_3 $\times 10^{-4}\text{GPa}^{-1}$	a_4 $\times 10^{-4}\text{GPa}^{-1}$	α	C_0 MPa	C_1 MPa
68	0.21	1.2565	393.71	-12.565	2.513	0.2309	0.001	0.55

Simulation 1: Initiation of Damage

Initiation of damage due to pressurization is simulated by assuming that the rock mass around the borehole is initially undamaged. FIG. 1&2 indicate that damage propagates into the rock mass within a zone increasing in size along both radial and axial directions. The damaged zone presents several symmetries in three dimensions, which are in agreement with the definition of the damage-driving force controlling the initiation and propagation of damage. A plot of the damage components (not shown here) also indicates that as expected, cracks open in planes perpendicular to the wellbore axis.

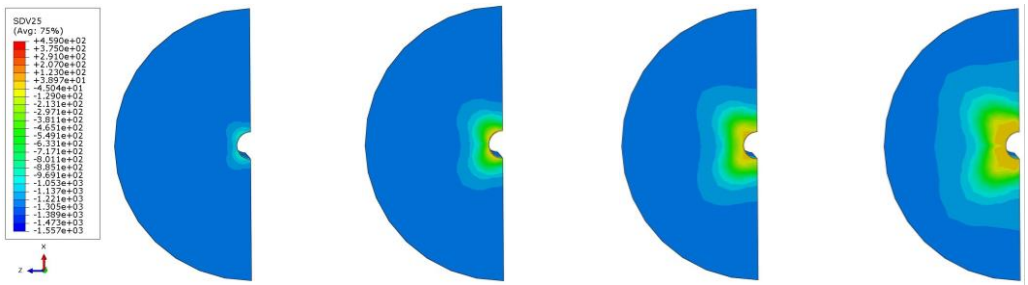

a). P=4MPa **b). P=28MPa** **c). P=78MPa** **d). P=200MPa**

FIG. 1 Damage zone evolution with pressures (transversal cross section)

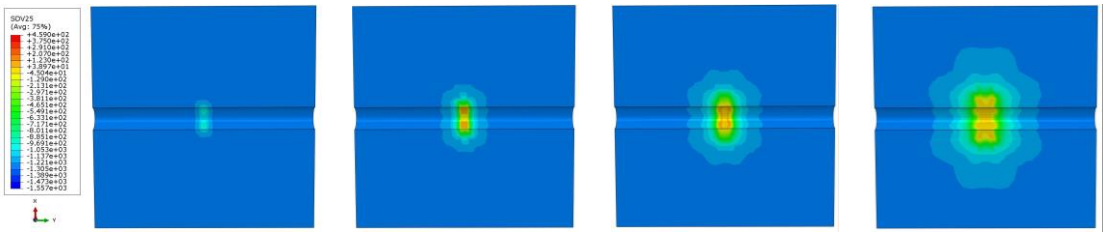

a). P=4MPa **b). P=28MPa** **c). P=78MPa** **d). P=200MPa**

FIG. 2 Damage zone evolution with pressures (axial cross section)

Simulation 2: Damage Propagation from Notches

In this second example, hydraulic fracturing is simulated under the assumption that notches at the wellbore walls were previously created to enhance fracture propagation during fluid injection. The geometry of the domain is kept unchanged, except for the presence of two conic notches, 0.2m in diameter (at the wellbore wall) and 0.7m in length. FIG. 4 shows the geometry of the initial defect.

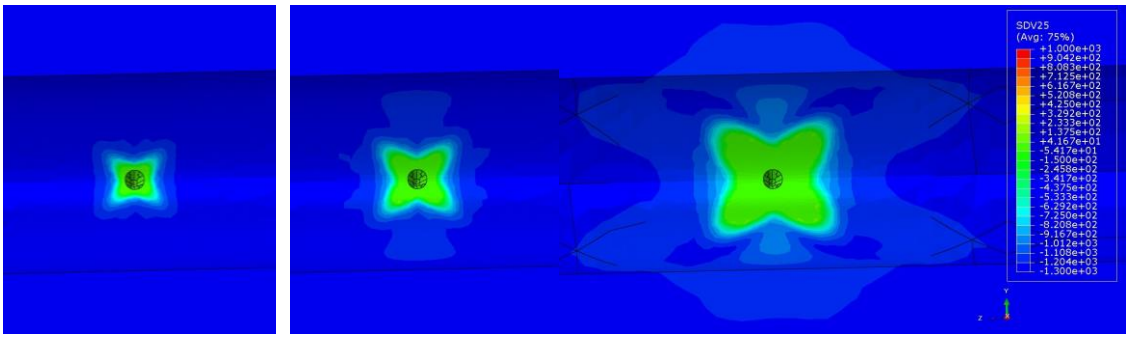

a). P=20MPa **b). P=50MPa** **c). P=178MPa**

FIG. 3 Damage zone evolution with pressures (zoom of wellbore axial section)

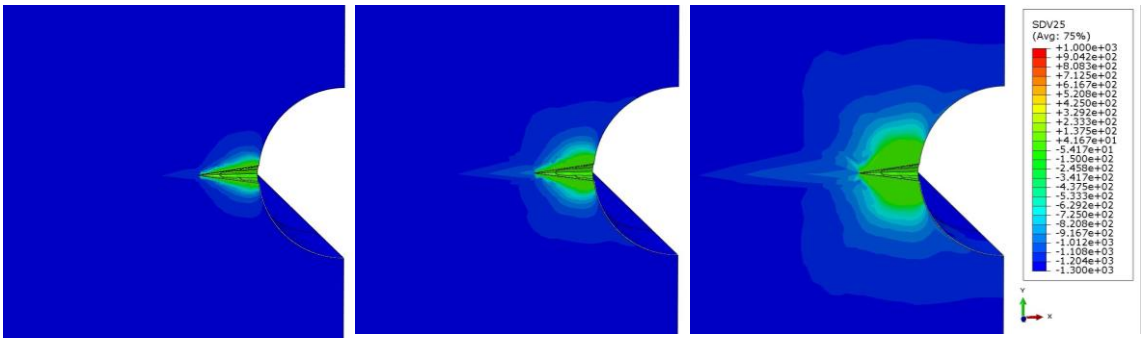

a). P=20MPa **b). P=50MPa** **c). P=178MPa**

FIG. 4 Damage zone evolution with pressures (zoom of transversal section)

The damage zone generated during the simulations is almost symmetric and localized near the notch (FIG. 3). Damage localizes around notch (FIG. 4a), and propagates radially (due to axis-symmetric conditions). For high pressures, damage tends to propagate ahead of the notch tip (FIG. 4b and 4c). In this second set of simulations, the surface of application of the normal pressure is much smaller than in the first set of simulation. The resulting damage driving force is therefore much smaller, so that under similar stress conditions, the extent of the damage zone is much smaller than in the previous set of simulations on damage initiation.

Simulation 3: Damage Propagation in a Smeared Damaged Zone

In the last example below, it is assumed that the rock mass has been pre-damaged mechanically (by explosion or by bullet projection for instance) in order to enhance hydraulic fracturing. Crack planes perpendicular to the axis of the wellbore are assumed to exist in the initial state (before fluid injection), in a zone spreading over

0.2m along the wellbore axis, and 0.7m in the radial direction. The initial damage component is set as $\Omega_{yy} = 0.05$ (y-direction is the vertical direction in the FIG. 5)

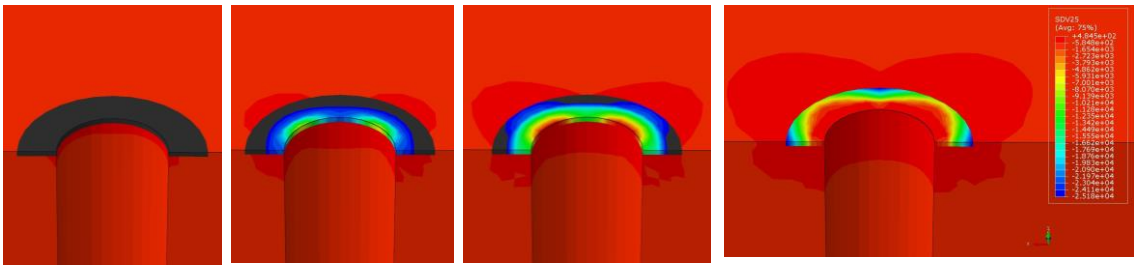

a). P=12MPa **b). P=50MPa** **c). P=80MPa** **d). P=200MPa**

FIG. 5 Damage zone evolution with pressures

The shape and extent of the new damage zone during pressurization is very similar to the one obtained in the first example (FIG. 5). However, because of the existence of initial cracks, rock mechanical response is different. According to the damage criterion used in the DSID model, initial damage tends to harden the rock. Therefore, it requires more mechanical energy to build up damage on the top of existing cracks. Damage generated during pressurization first concentrates around the initial damage zone (FIG. 5a). This phenomenon represents well what would happen in the viscosity-dominated propagation regime of hydraulic fractures (Savitski and Detournay, 2002): pre-existing cracks tend to open without growing. Once damage ahead of the damage zone starts to initiate (FIG. 5b), damage propagates very rapidly in the radial direction, because the damage threshold (to open new cracks) is low in pristine rock (FIG. 5c and 5d). This part of the simulation reproduces what would occur after the viscosity-dominated propagation regime: once the lag between the fluid propagation front and the fracture tip becomes negligible, rock toughness is the parameter controlling hydraulic fracture propagation. The final damaged zone obtained in this third example is not localized like in the second example. Therefore, it can be concluded that simulating pre-existing damage by setting a non-zero value for the damage tensor is an efficient way to link fracture propagation problems at the borehole and continuum scales.

CONCLUSION

A Continuum Damage Mechanics (CDM) model is presented to improve the prediction of rock stiffness in the damaged zone surrounding hydraulic fractures. At the scale of the Representative Elementary Volume (REV), damage is assumed to propagate in mode I (in fact the model represents splitting and crossing microscopic processes, i.e. micro-crack propagation in modes I and II). The proposed "Differential Stress Induced Damage" (DSID) model was implemented in *ABAQUS* Finite Element code in order to map stress and degradation of rock mass stiffness at the reservoir scale. Localized pressurization from a wellbore was simulated. In a pristine rock mass, the damage zone presents several symmetries in three dimensions, which are in agreement with the definition of the damage-driving force controlling the initiation and propagation of damage. If hydraulic fracturing is enhanced by the presence of initial cracks, the propagation of the damage zone depends on the geometry of the initial defects. The

presence of notches tends to reduce the surface of application of the pressure causing damage. As a result the damage driving force stays relatively small and the damage zone localizes around the notch, even under high pressures gradients. In the presence of a smeared damage zone, damage first concentrates around the initial damage zone (analog of the viscosity-dominated propagation regime). Once damage ahead of the damage zone starts to initiate, damage propagates very rapidly in the radial direction, because the damage threshold (to open new cracks) is low in pristine rock (analog of the toughness-dominated propagation regime). Simulating pre-existing damage by setting a non-zero value for the damage tensor turns to be an efficient way to link fracture propagation problems at the borehole and continuum scales. The ultimate goal of this research work is to formulate a continuum-based model of hydraulic fracturing. A remaining challenging issue consists in capturing the interaction between fracture propagation and rock mass hydro-mechanical behavior (including damaged stiffness and damaged permeability).

ACKNOWLEDGMENTS

This research was performed in the School of Civil and Environmental Engineering at the Georgia Institute of Technology, with the support of ConocoPhillips on a project entitled "Finite Element Modeling of Hydraulic Fracturing".

REFERENCES

Adachi, J., Siebrits, E., Peirce, A. and Desroches, J. (2007) "Computer simulation of hydraulic fractures." *International Journal of Rock Mechanics and Mining Sciences*, Vol. 44:739-757.

Carrier, B. and Granet, S. (2012). "Numerical modeling of hydraulic fracture problem in permeable medium using cohesive zone model." *Engineering Fracture Mechanics,* Vol. 79: 312–328.

Cicekli, U., Voyiadjis, G.Z. and Abu Al-Rub, R.K. (2007). "A plasticity and anisotropic damage model for plain concrete." *International Journal of Plasticity*, Vol. 23: 1874-1900.

Colovos, J.W., Brannon, R.B. and Pinsky, P.M. (2013). "Reduction of macroscale calibration experiments through constraints on anisotropic elastic stiffnesses." *Proceedings of the 47th US Rock Mechanics/Geomechancis Symposium*, 23-26 June 2013, San Francisco, California, paper ID: 13-656.

Cowin, S.C. (1985). "The relationship between the elasticity tensor and the fabric tensor." *Mechanics of Materials*, Vol. 4:137-147.

Florez-Nino, J-.M, Aydin, A., Mavko, G., Antonellini, M. and Ayaviri, A. (2005). "Fault and fracture systems in a fold and thrust belt: An example from Bolivia." *AAPG Bulletin*, Vol. 89(4): 471–493.

Halm, D. and Dragon, A. (1998). "An anisotropic model of damage and frictional sliding for brittle materials." *Eur. J. Mech. A/ Solids*, Vol. 17(3): 439-460.

Kachanov, M. (1992). "Effective elastic properties of cracked solids: critical review of som basic concepts." *Appl. Mech. Rev.*, Vol. 45(8): 304-335.

Lemaitre, J. and Desmorat, R. (2005) *Engineering Damage Mechanics. Ductile, creep,*

fatigue and brittle failure. Springer - Verlag, Berlin Heidelberg.

Liu, H.W. (1984). "On the fundamental basis of fracture mechanics." *Engineering Fracture Mechancis*, Vol. 17(5): 425-438.

Lubarda, V.A. and Krajcinovic, D. (1993). "Damage tensors and the crack density distribution." *International Journal of Solids and Structures*, Vol. 30(20): 2659-2677.

Maleki, K. and Pouya, A. (2010). "Numerical simulation of damage-Permeability relationship in brittle geomaterials." *Computers and Geotechnics*, Vol. 37(5): 619-628.

Oda., M. (1984). "Similarity rules of crack geometry in statistically homogeneous rock masses." *Mechanics of Materials*, Vol. 3:119-129.

Savitski, A. and Detournay, E. (2002). "Propagation of a penny-shaped fluid-driven fracture in an impermeable rock: asymptotic solutions." *International Journal of Solids and Structures*, Vol. 39:6311-6337.

Shao, J.-F., Zhou, H. and Chau, K.T. (2005). "Coupling between anisotropic damage and permeability variation in brittle rocks." *International Journal for Numerical and Analytical Methods in Geomechanics*, Vol. 29: 1231-1247.

Suzuki, T. (2012). "Understanding of dynamic earthquake slip behavior using damage as a tensor variable: Microcrack distribution, orientation, and mode and secondary faulting." *Journal of Geophysical Research*, Vol. 117(B5):1-20.

Swoboda, G. and Yang, Q. (1999). "An energy-based damage model of geomaterials -II. Deduction of damage evolution laws." *International Journal of Solids and Structures*, Vol. 36:1735-1755.

Tarokh, A. and Fakhimi, A. (2013). "Relationship between grain size and fracture properties of rock." *Proceedings of the 47th US Rock Mechanics/Geomechancis Symposium*, 23-26 June 2013, San Francisco, California, paper ID: 13-168.

Tsang, C-.F., Bernier, F. and Davies, C. (2005). "Geohydromechanical processes in the Excavation Damaged Zone in crystalline rock, rock salt, and indurated and plastic clays—in the context of radioactive waste disposal." *International Journal of Rock Mechanics & Mining Sciences*, Vol. 42: 109–125.

Ulm, F.J., Dormieux, L. and Kondo, D. (2006). *Microporomechanics.* John Wiley & Sons.

Valko, P. and Economides, M.J. (1994). "Propagation of hydraulically induced fractures a Continuum Damage Mechanics approach." *International Journal of Rock Mechanics and Mining Sciences & Geomechanics Abstracts*, Vol. 31(3): 221-229.

Xu, H. and Arson, C. (2014). "Anisotropic Damage Models for Geomaterials: Theoretical and Numerical Challenges", *International Journal of Computational Methods, Special Issue on Computational Geomechanics*, Vol. 11 (2) (in press)